Journal of Electromagnetic Analysis and Applications, 2023, 15, 43-58
https://www.scirp.org/journal/jemaa
ISSN Online: 1942-0749
ISSN Print: 1942-0730

Generation of Higher Terahertz Harmonics in Nonlinear Paraelectrics under Focusing in a Wide Temperature Range

Volodymyr Grimalsky[1], Jesus Escobedo-Alatorre[1], Christian Castrejon-Martinez[2], Yered Gomez-Badillo[1]

[1]Center for Investigations on Engineering and Applied Science (CIICAp), Institute for Investigations on Basic and Applied Science (IICBA), Autonomous University of State Morelos (UAEM), Cuernavaca, Mor., Mexico
[2]Tecnológico Nacional de México/Instituto Tecnológico de Zacatepec, Zacatepec, Mor., Mexico
Email: v_grim@hotmail.com, jescobedo@uaem.mx, christian.cm@zacatepec.tecnm.mx

How to cite this paper: Grimalsky, V., Escobedo-Alatorre, J., Castrejon-Martinez, C. and Gomez-Badillo, Y. (2023) Generation of Higher Terahertz Harmonics in Nonlinear Paraelectrics under Focusing in a Wide Temperature Range. *Journal of Electromagnetic Analysis and Applications*, **15**, 43-58.
https://doi.org/10.4236/jemaa.2023.154004

Received: January 26, 2023
Accepted: April 25, 2023
Published: April 28, 2023

Abstract

It is theoretically investigated the generation of higher harmonics of two-dimensional and three-dimensional terahertz electromagnetic beams in nonlinear crystals. The attention is paid to crystalline paraelectrics like $SrTiO_3$ under the temperatures 60 - 200 K, these crystals possess the cubic nonlinearity. The bias electric field is applied to provide the dominating quadratic nonlinearity. The initial focusing of the beams not only increases the efficiency of generation of higher harmonics, but alto makes possible to select maxima of different higher harmonics at some distances from the input. At lower temperatures the nonlinearity behaves at smaller input amplitudes, whereas at higher temperatures the harmonic generation can be observed at higher frequencies up to 1.5 THz. In three-dimensional beams the peak amplitudes of higher harmonics can be bigger than in two-dimensional beams, but the ratios of these peak values to the maximum values of the focused first harmonic are smaller than in two-dimensional beams.

Keywords

Terahertz Wave Beams, Nonlinear Crystalline Paraelectrics, Different Temperatures, Generation of Harmonics, Initial Focusing

1. Introduction

Now the assimilation of the terahertz (THz) range 0.1 - 30 THz takes place [1]-[17]. As the nonlinear crystals, the ferroelectrics in the non-polar phase are utilized as the nonlinear dielectrics in the lower part of THz range, so-called pa-

raelectrics like $SrTiO_3$, $KTaO_3$ [18]-[40]. The crystalline $SrTiO_3$ possesses high cubic electrodynamic nonlinearity and low losses in the lower part of THz range 0.1 - 2.5 THz at moderately low temperatures $T = 60$ - 200 K. There exists the frequency dispersion in THz range when the frequency is near the soft mode frequency *i.e.* the lowest frequency of oscillations of the optical type of the crystalline lattice [19] [21] [22] [23] [24] [27] [28] [40] [41] [42]. In the crystalline $SrTiO_3$ the soft mode frequency decreases with the decrease of the temperature whereas the dielectric nonlinearity increases there [19]. In the absence of the frequency dispersion in the microwave range, the nonlinearity results in the generation of higher harmonics and forming the shock electromagnetic (EM) waves [29] [30]. The waveguide dispersion can be used there [31].

Because there is a problem of excitation of powerful THz radiation, the interesting and important phenomenon is generation of higher harmonics [33] [39] of input EM waves at relatively low frequencies. The transverse bias electric field should be applied to provide the induced quadratic nonlinearity [29] [33]. Earlier the generation of higher THz harmonics was investigated in 2D geometry, or for the beams that depend on a single transverse coordinate, at the temperature $T \approx 80$ K [33]. Only the quadratic nonlinearity was taken into account there. Note that the frequencies of higher harmonics are limited by the soft mode frequency. At higher temperatures the soft mode frequency increases, whereas the nonlinearity decreases. Therefore, for the practical needs it is rather better to investigate the generation of higher harmonics in the wide temperature interval. In THz range the dissipation in the paraelectrics increases compared with the microwave range. A possible way to compensate losses is using the initial focusing of the EM wave beams [33] [34] [36] [37] [39]. Thus, also 3D THz beams should be considered to produce better initial focusing. Under maximum concentration of EM energy in 3D case, the role of the cubic nonlinearity may be essential compared with 2D case, as well as the self-action due the generation of the zeroth harmonic. The cubic nonlinearity results in both the influence on generation of higher harmonics and in the self-action.

The present paper is devoted to the theoretical investigations of generation of higher harmonics of THz EM waves in paraelectric crystals like $SrTiO_3$ in the wide temperature range $T = 60$ - 200 K. The bias electric field is applied to provide the dominating quadratic nonlinearity. The terms due to the cubic nonlinearity are taken into account, too. Both the focusing of 2D, or plane, beams and 3D, or cylindrical, ones are considered. At lower temperatures the dielectric nonlinearity is higher, but the possible frequency range is lower due to decreasing the soft mode frequency. At higher temperatures, it is possible to increase the frequency range. It is demonstrated that the cubic nonlinearity is not important under focusing of 2D beams, but it is important under extreme focusing of 3D beams.

2. Basic Equations

The nonlinear propagation of EM wave beams with the dominating electric field

component $E_y = E$ is considered along OZ axis within the crystalline paraelectric $SrTiO_3$. The dielectric nonlinearity in $SrTiO_3$ is due to the nonlinear properties of the lattice polarization $\varepsilon_0 P$, where ε_0 is the electric constant, SI units. Both the cases of plane, or 2D, beams $E_y(t, x, z)$ and symmetrical cylindrical, or 3D, ones $E_y(t, \rho, z)$ are investigated. The basic equations that describe the nonlinear EM wave propagation in paraelectric crystalline $SrTiO_3$ are [18] [19] [26] [32] [33]:

$$\begin{aligned}
&\frac{\partial^2 P}{\partial t^2} + \gamma \frac{\partial P}{\partial t} + \omega_T^2 \left(1 + \frac{P^2}{P_n^2}\right) P = \varepsilon(0)\omega_T^2 E;\\
&\frac{\partial^2 E}{\partial z^2} + \Delta_\perp E = \frac{1}{c^2}\frac{\partial^2 P}{\partial t^2};\\
&D \equiv \varepsilon_0 (E + P) \approx \varepsilon_0 P;\\
&\Delta_\perp E \equiv \begin{cases} \dfrac{\partial^2 E}{\partial x^2} & \text{in 2D case,} \\ \dfrac{1}{\rho}\dfrac{\partial}{\partial \rho}\left(\rho \dfrac{\partial E}{\partial \rho}\right) & \text{in 3D case;} \end{cases}\\
&\rho \equiv \left(x^2 + y^2\right)^{1/2}.
\end{aligned} \tag{1}$$

Below both 3D beams and 2D ones are considered. Here ω_T is the soft mode frequency, which is in THz range for $SrTiO_3$, γ is the lattice dissipation. At the temperature $T \approx 80$ K it is $\omega_T \approx 6 \times 10^{12}\ \mathrm{s}^{-1}$, and the static linear dielectric permittivity is $\varepsilon(0) \equiv \varepsilon(\omega = 0) = 1.8 \times 10^3$ [19] [26] [33]. In paraelectric crystalline $SrTiO_3$ the permittivity increases with the decrease of temperature. In Equations (1) the parameter P_n determines the value of the cubic nonlinearity of the polarization. It is connected with the characteristic magnitude of the electric field E_0, where the nonlinearity is essential: $P_n = \varepsilon(0) E_n$. At the temperature $T \approx 80$ K it is $E_n = 60$ kV/cm [19] [26]. The cubic nonlinearity is proportional to $\varepsilon(0)^3$, *i.e.* $E_n \sim \varepsilon(0)^{-3/2}$. Because of small dissipation in $SrTiO_3$, the nonlinearity manifests at the amplitudes of EM waves at least one order smaller than E_n. The parameters of $SrTiO_3$ used in simulations are presented in **Figure 1**.

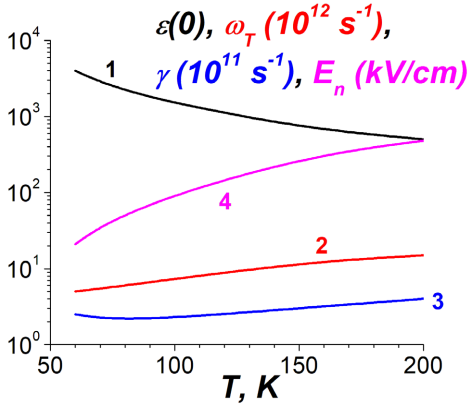

Figure 1. The temperature dependencies of the static linear permittivity $\varepsilon(0)$, curve 1; of the soft mode frequency ω_T (10^{12} s^{-1} units), curve 2; of the lattice dissipation γ (10^{11} s^{-1} units), curve 3; and of the nonlinear parameter E_n (kV/cm), curve 4.

For 3D, or cylindrical, EM beams the validity of the paraxial approximation is assumed and checked [37], namely the possible focusing is moderate and the longitudinal component of the electric field is small $|E_z| \ll |E_y|$.

In the linear case Equations (1) result in the well-known expressions of the complex dielectric permittivity $\varepsilon(\omega) \equiv \varepsilon'(\omega) + i\varepsilon''(\omega)$ and to the dispersion relation for the plane EM wave $k = k(\omega)$ [19] [26] [33]:

$$\varepsilon(\omega) \approx \frac{\varepsilon(\omega=0)\cdot\omega_T^2}{\omega_T^2 - \omega^2 + i\gamma\omega},\ \omega > 0;$$
$$k(\omega) \equiv k' + ik'' = \frac{\omega}{c}\varepsilon(\omega)^{1/2};\ E \sim \exp\left(i(\omega t - kz)\right). \tag{2}$$

In the nonlinear stationary case Equations (1) result in the known formula for the nonlinear permittivity [19] [26]:

$$\varepsilon(E) = \frac{\varepsilon(\omega=0)}{1+\frac{P^2}{P_n^2}} \approx \frac{\varepsilon(\omega=0)}{1+\frac{E^2}{E_n^2}} \approx \varepsilon(\omega=0)\left(1-\frac{E^2}{E_n^2}\right). \tag{3}$$

Equations (3) for the static nonlinear permittivity are equivalent in the case of moderate electric fields $|E| < E_n$, that is considered below.

3. Equations for Slowly Varying Amplitudes

Here the nonlinear EM wave propagation is investigated in the crystalline $SrTiO_3$, when the bias electric field E_s is applied [33]:

$$E = E_s + \tilde{E},\ P = P_s + \tilde{P};$$
$$P_s \cdot \left(1+\frac{P_s^2}{P_n^2}\right) = \varepsilon(0)\omega_T^2 E_s. \tag{4}$$

In the absence of the bias field only the odd harmonics are excited, and the efficiency is low, as our simulations have been demonstrated. In the presence of the bias field the induced quadratic nonlinearity becomes dominating, but the cubic nonlinearity should be preserved generally in the equations. Generally all harmonics, even and odd ones, are essential. The equations for the variable components of the polarization $\tilde{P}$ and the electric field $\tilde{E}$ are:

$$\frac{\partial^2\tilde{P}}{\partial t^2} + \gamma\frac{\partial\tilde{P}}{\partial t} + \tilde{\omega}_T^2\tilde{P} + \omega_T^2\left(\frac{3P_s\tilde{P}^2}{P_n^2} + \frac{\tilde{P}^3}{P_n^2}\right) = \varepsilon(0)\omega_T^2\tilde{E};$$
$$\Delta\tilde{E} \equiv \frac{\partial^2\tilde{E}}{\partial z^2} + \Delta_\perp\tilde{E} = \frac{1}{c^2}\frac{\partial^2\tilde{P}}{\partial t^2};\ \tilde{\omega}_T^2 \equiv \omega_T^2\left(1+\frac{3P_s^2}{P_n^2}\right). \tag{5}$$

From Equations (5) it is possible to obtain a single equation for the polarization [33]:

$$\Delta\left(\frac{\partial^2\tilde{P}}{\partial t^2} + \gamma\frac{\partial\tilde{P}}{\partial t} + \tilde{\omega}_T^2\tilde{P}\right) - \frac{\omega_T^2}{c^2}\varepsilon(0)\frac{\partial^2\tilde{P}}{\partial t^2}$$
$$= -\omega_T^2\left(\frac{3P_s}{P_n^2}\Delta\left(\tilde{P}^2\right) + \frac{1}{P_n^2}\Delta\left(\tilde{P}^3\right)\right). \tag{6}$$

The nonlinearity is considered as moderate here, and the method of slowly varying amplitudes is applied [33] [43] [44] [45].

Below the propagation of THz EM beams along *OZ* axis is considered. The solution of Equation (6) is searched as the set of harmonics including the zeroth harmonic:

$$\begin{aligned}&\tilde{P}=\frac{1}{2}\sum_{j=1,2,3,\cdots}B_j\left(z,\vec{r}_\perp,t\right)\mathrm{e}^{i\varphi_j}+c.c.+B_0\left(z,\vec{r}_\perp,t\right);\\&\varphi_j\equiv\omega_j t-k'\left(\omega_j\right)z;\ \ \omega_j=j\cdot\omega_1;\\&k\left(\omega\right)\equiv k'+ik''=\frac{\omega}{c}\varepsilon\left(\omega\right)^{1/2},\ \ \varepsilon\left(\omega\right)\approx\frac{\varepsilon\left(\omega=0\right)\cdot\omega_T^2}{\tilde{\omega}_T^2-\omega^2+i\gamma\omega}.\end{aligned}\tag{7}$$

Here $B_j(z, r_\perp, t)$ are the slowly varying amplitudes of harmonics for the polarization; ω, k are the carrier frequencies and the corresponding linear wave numbers of EM wave [33]. It is seen that the bias electric field E_s and thus the polarization P_s change the linear permittivity $\varepsilon(\omega)$) and the dispersion relation for EM waves $k = k(\omega)$ due to the presence of $\tilde{\omega}_T > \omega_T$ there.

The frequency dependencies of the real parts of the permittivity, the real and imaginary parts of wave numbers of EM waves, and the ratios of the imaginary part to the real one of the permittivity are given in **Figure 2**. The bias field $E_s = 0.3E_n$ is applied; the proper values of the characteristic nonlinear field are taken for each temperature, see **Figure 1**.

In Equations (7) the zeroth harmonic term is taken into account that is due to the induced quadratic nonlinearity. From Equation (6) it is possible to obtain the following expression for B_0:

$$\tilde{\omega}_T^2B_0+\frac{3P_s}{2P_n^2}\omega_T^2\sum_{l=1,2,3,\cdots}\left|B_l\right|^2=0.\tag{8}$$

In another words, the term with $B_0 < 0$ results in the effective decreasing of the bias polarization P_s, *i.e.*

$$P_s\to P_s\cdot\left(1-\frac{3\omega_T^2}{2P_n^2\tilde{\omega}_T^2}\sum_{l=1,2,3,\cdots}\left|B_l\right|^2\right).\tag{9}$$

With using the standard procedure described in details in [33], the following nonlinear parabolic equations for harmonics have been derived:

$$\begin{aligned}&\frac{\partial B_j}{\partial z}+\frac{i}{2k_j'}\Delta_\perp B_j+\Gamma_jB_j\\&=\frac{ik_j'\omega_T^2}{\left(\tilde{\omega}_T^2-\omega_j^2+i\gamma\omega_j\right)P_n^2}\left\{\frac{3P_s}{4}\left[\sum_mB_mB_{j-m}\exp\left(i\left(\varphi_m+\varphi_{j-m}-\varphi_j\right)\right)\right.\right.\\&\left.+2\sum_mB_m^*B_{j+m}\exp\left(i\left(-\varphi_m+\varphi_{j+m}-\varphi_j\right)\right)+4B_0B_j\right]\\&+\frac{1}{8}\left[\sum_{m,p}B_{j-m-p}B_mB_p\exp\left(i\left(\varphi_m+\varphi_p+\varphi_{j-m-p}-\varphi_j\right)\right)\right.\\&+3\sum_{m,p}B_{m+p-j}^*B_mB_p\exp\left(i\left(\varphi_m+\varphi_p-\varphi_{m+p-j}-\varphi_j\right)\right)\\&\left.\left.+3\sum_{m,p}B_{m+p+j}B_m^*B_p^*\exp\left(i\left(\varphi_m+\varphi_p-\varphi_{m+p-j}-\varphi_j\right)\right)\right]\right\}.\end{aligned}\tag{10}$$

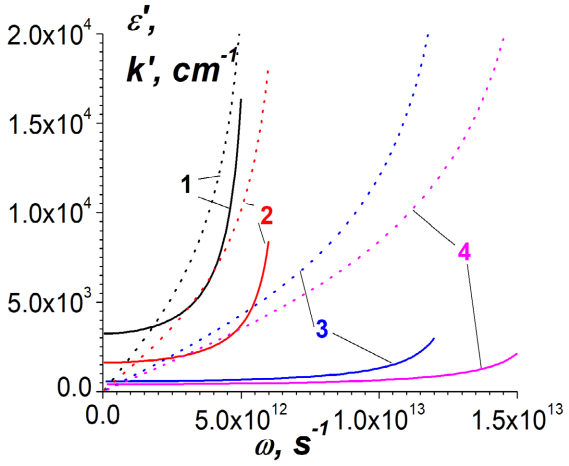

(a)

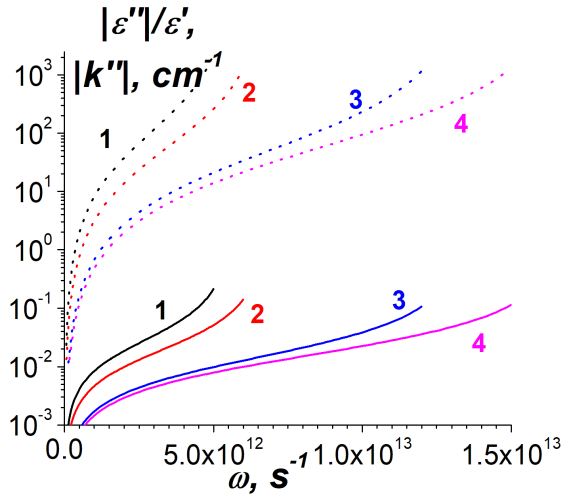

(b)

Figure 2. The dependencies on frequency ω of the parameters of THz waves in the crystalline $SrTiO_3$. Part (a) is the dependencies of the real parts of the linear permittivity ε', solid curves, and the wave numbers of EM wave k', dot curves. Part (b) is the dependencies of the imaginary part of the wave number k'', dot curves, and $\tan(\delta) \equiv |\varepsilon''|/\varepsilon'$, solid curves. The curves 1, 2, 3, 4 are at the temperatures $T = 60$ K, 77 K, 150 K, and 200 K correspondingly. The bias electric field is $E_s = 0.3E_n$.

For simulations it is better to rewrite Equations (10) with using the slowly varying amplitudes for harmonics A_j of the electric field $\check{E}$. From the second Equation (5) there is the relation

$$\begin{aligned} &\left(k_j'\right)^2 A_j \exp\left(-ijk_1'z\right) = \frac{\omega_j^2}{c^2} B_j \exp\left(-ik_j'z\right); \\ &\text{or } B_j = \varepsilon(0)\alpha_j A_j \exp\left(i\left(k_j' - jk_1'\right)z\right); \\ &\alpha_j \equiv \frac{1}{\varepsilon(0)}\left(\frac{k_j'c}{\omega_j}\right)^2 \approx 1. \end{aligned} \tag{11}$$

From Equation (11) the following set of equation is written down:

$$\frac{\partial A_j}{\partial z}+\frac{i}{2k_j'}\Delta_\perp A_j+i\left(k_j-jk_1'\right)A_j$$
$$=i\frac{k_j'\omega_T^2\varepsilon^2(0)}{\left(\tilde{\omega}_T^2-\omega_j^2+i\gamma\omega_j\right)P_n^2\alpha_j}\left\{\frac{3P_s}{4\varepsilon(0)}\left[\sum_m\alpha_{j-m}\alpha_m A_{j-m}A_m\right.\right.$$
$$\left.+2\sum_m\alpha_{m-j}\alpha_m A_{m-j}^*A_m+4A_0\alpha_j A_j\right]$$
$$+\frac{1}{8}\left[\sum_{m,p}\alpha_{j-m-p}\alpha_m\alpha_p A_{j-m-p}A_mA_p+3\sum_{v,p}\alpha_{m+p-j}\alpha_m\alpha_p A_{m+p-j}^*A_mA_p\right.$$
$$\left.\left.+3\sum_{v,p}\alpha_{j+m-p}\alpha_m\alpha_p A_{j+m+p}A_m^*A_p^*\right]\right\};\ P_n/\varepsilon(0)\equiv E_n,\ P_s/\varepsilon(0)\approx E_s. \tag{12}$$

In Equations (12) the expression for the zeroth harmonic A_0 is

$$A_0\equiv\frac{B_0}{\varepsilon(0)}=-\frac{3P_s\varepsilon(0)\omega_T^2}{2P_n^2\tilde{\omega}_T^2}\sum_{l=1,2,3,\cdots}\alpha_l^2\left|A_l\right|^2. \tag{13}$$

It is assumed that the first harmonic only is at the input of the system, $\omega_1 < \omega_T/10$. All higher harmonics and the zeroth one are excited by the nonlinearity. It is possible to excite the higher harmonics at the frequencies $\omega_j \geq 0.5\omega_T$, as our simulations have demonstrated.

To increase the efficiency of generation of higher harmonics, the initial focusing by the circular antenna is applied, see Figure 3. The boundary condition for the first harmonic is in 2D case

$$A_1\left(z=0,x,t\right)=A_{10}F_x\left(x\right)M\left(x\right). \tag{14}$$

In 3D case there is the radial distance ρ instead x. Here A_{10} is the maximum value of the amplitude at the input $z = 0$, the transverse profile is $F_x(x)$. This transverse profile is assumed as almost rectangular with the width x_0 or ρ_0. At the output the matching load is assumed, *i.e.* there are no reflections there.

The factor $M(x)$ is due to a possible initial focusing of the pulse due to the excitation of the circular antenna, see Figure 3. It is considered the symmetrical case with respect to $x = 0$.

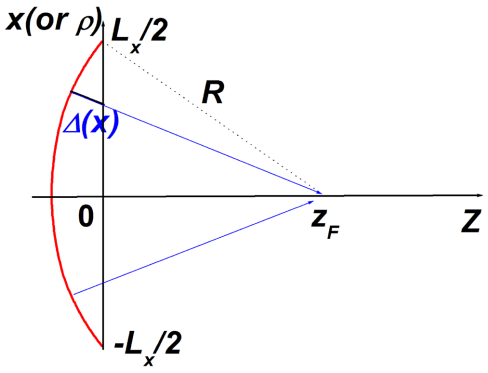

Figure 3. Possible initial focusing of THz beams due to the circular antenna. The symmetric case is considered with respect to $x = 0$. In 3D axially symmetric case the transverse coordinate is ρ.

At the input of the nonlinear crystal $z = 0$ the EM wave gets the phase shift $-k\Delta(x) = -k\left(R - \left(z_c^2 + x^2\right)^{1/2}\right)$, where z_c is the distance from the input to the focus point $z_c = \left(R^2 - \left(L_x/2\right)^2\right)^{1/2}$, k is the wave number; thus the phase multiplier is $M(x) = \exp\left(-ik\Delta(x)\right)$. In 3D case x is replaced by the radial coordinate ρ.

4. Simulations of Generation of Harmonics

The simulations of generation of higher harmonics in the nonlinear crystal $SrTiO_3$ have been realized under different temperatures, both in 2D and 3D geometries. It has been obtained that the pure cubic nonlinearity without the bias electric field is not effective for this generation. There is the optimum value of the bias electric field $E_s \approx (0.2 - 0.4)E_n$ to realize the generation of higher harmonics. At smaller values the induced quadratic nonlinearity is small whereas at higher values $E_s \geq 0.5E_n$ the saturation of nonlinearity occurs and the efficiency of the generation does not increase, as seen from Equation (4). For all the cases considered below it is chosen $E_s = 0.3E_n$ where E_n is the characteristic nonlinear electric field under each temperature. The length of the nonlinear crystal is $L_z =$ 0.5 cm. The parameters of the nonlinear crystal at different temperatures are given in Table 1, see also Figure 1.

The numerical simulations have been provided by the implicit finite difference schemes [46]. Several iterations have been applied that demonstrate good convergence. The simulations have demonstrated a possibility of generation of higher harmonics with the numbers $n \geq 5$, *i.e.* the frequency multiplication, or frequency up-conversion, in the whole temperature interval $T = 60 - 200$ K.

The typical results of simulations are presented in Figures 4-8. It is seen that in the focused beams the maxima of different higher harmonics are realized at different distances from the input of the crystal.

At lower temperatures the nonlinearity is higher, so the input amplitudes of the first harmonics can quite lower, of about 1 kV/cm. But the highest frequencies that can be obtained under the up-conversion are of about 0.5 THz. In turn, at higher temperatures it is possible to excite the frequencies up to $f \equiv \omega/2\pi = 1.5$ THz.

From our simulations in is seen that the concentration of the energy near the focus is naturally higher in 3D beams. For this reason, in 2D beams the influence

Table 1. The used parameters of crystalline $SrTiO_3$.

T, K	$\varepsilon(0)$	ω_T, 10^{12} s^{-1}	γ, 10^{11} s^{-1}	E_n, 10^4 V/cm
60	4000	5	2.5	2.1
77	2000	6	2	6
150	700	12	3	29
200	500	15	4	48

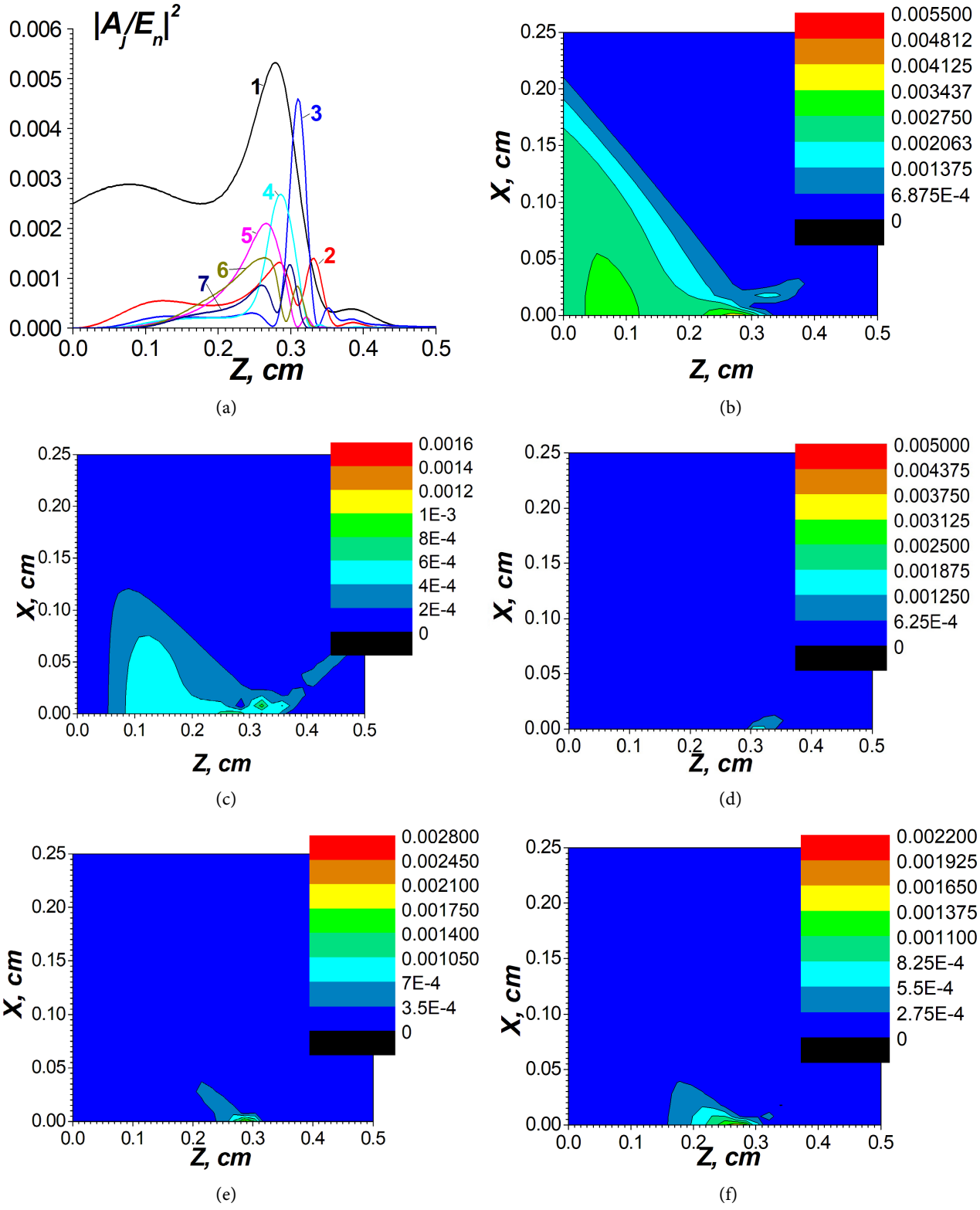

Figure 4. The generation of higher harmonics under the temperature $T = 60$ K in 2D beam. Part (a) is the longitudinal dependences of $|A_j(z)/E_n|^2$ in the center of the crystal $x = 0$. The dependencies are given for 7 harmonics. Parts (b) - (f) are distributions of $|A_j(x, z)/E_n|^2$ for harmonics with numbers $j = 1, 2, 3, 4, 5$ correspondingly. The parameters of 2D beam are as follows, the amplitude of the first harmonic is $A_{10} = 0.05E_n$, the initial transverse width of the beam is $x_0 = 0.44$ cm, the frequency of the first harmonic is $\omega_1 = 2 \times 10^{11}$ s^{-1}, the radius of the focusing antenna is $R = 0.35$ cm.

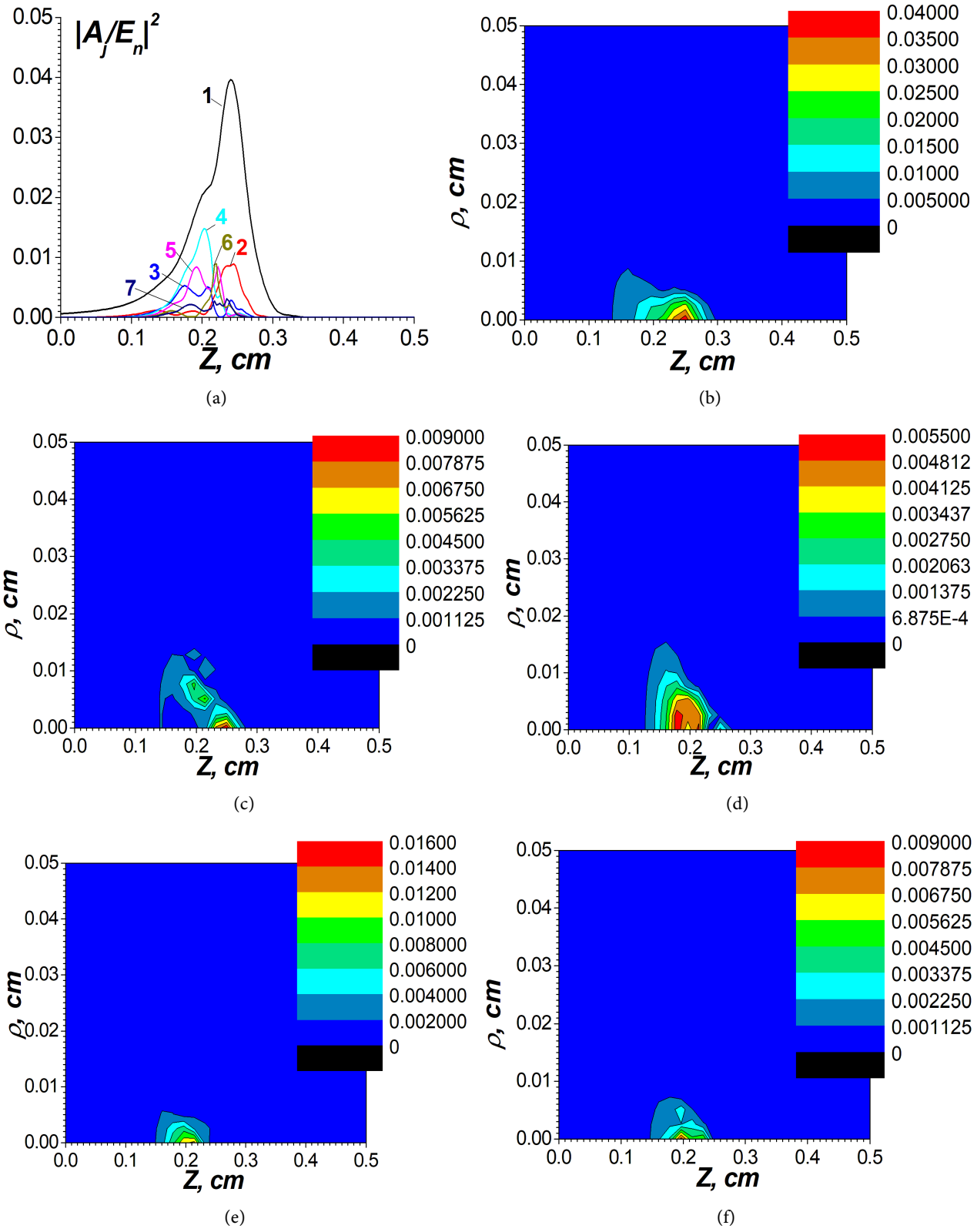

Figure 5. The generation of higher harmonics under the temperature $T = 60$ K in 3D beam. Part (a) is the longitudinal dependences of $|A_j(z)/E_n|^2$ in the center of the crystal $\rho = 0$. Parts (b) - (f) are distributions of $|A_j(x, z)/E_n|^2$ for harmonics with numbers $j = 1, 2, 3, 4, 5$ correspondingly. The parameters of 3D beam are $A_{10} = 0.025E_n$, $\rho_0 = 0.44$ cm, $\omega_1 = 3 \times 10^{11}$ s^{-1}, the radius of the focusing antenna is $R = 0.3$ cm.

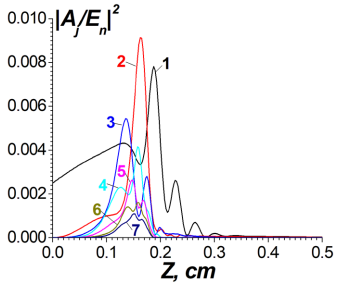

(a)

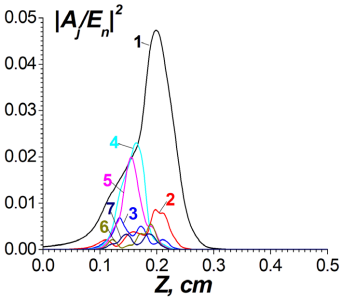

(b)

Figure 6. The generation of higher harmonics under the temperature $T = 77$ K. The longitudinal dependences of $|A_j(z)/E_n|^2$ in the center of the crystal are given. Part (a) is for 2D beam, part (b) is for 3D beam. The parameters of beams are $A_{10} = 0.05E_n$ for 2D beam and $A_{10} = 0.025E_n$ for 3D beam, $x_0 = \rho_0 = 0.44$ cm, $\omega_1 = 4 \times 10^{11}$ s^{-1}, the radius of the focusing antenna is $R = 0.28$ cm.

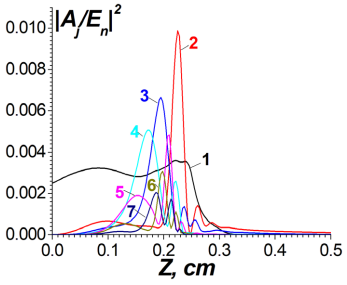

(a)

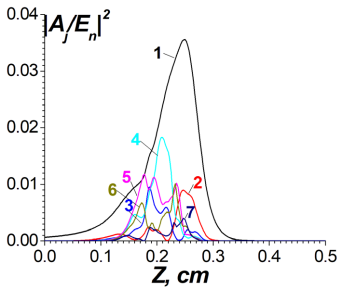

(b)

Figure 7. The generation of higher harmonics under the temperature $T = 150$ K. The longitudinal dependences of $|A_j(z)/E_n|^2$ in the center of the crystal are given. Part (a) is for 2D beam, part (b) is for 3D beam. The parameters of beams are $A_{10} = 0.05E_n$ for 2D beam and $A_{10} = 0.025E_n$ for 3D beam, $x_0 = \rho_0 = 0.44$ cm, $\omega_1 = 6 \times 10^{11}$ s^{-1}, the radius of the focusing antenna is $R = 0.3$ cm.

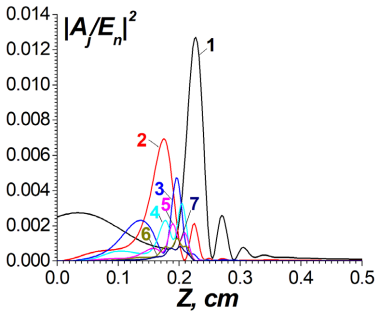

(a)

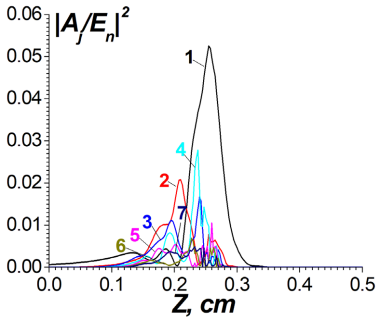

(b)

Figure 8. The generation of higher harmonics under the temperature $T = 200$ K. The longitudinal dependences of $|A_j(z)/E_n|^2$ in the center of the crystal are given. Part (a) is for 2D beam, part (b) is for 3D beam. The parameters of beams are $A_{10} = 0.05E_n$ for 2D beam and $A_{10} = 0.025E_n$ for 3D beam, $x_0 = \rho_0 = 0.44$ cm, $\omega_1 = 1 \times 10^{12}$ s^{-1}, the radius of the focusing antenna is $R = 0.3$ cm.

of the cubic nonlinearity and the zeroth harmonic is not essential. In 3D beams this influence should be taken into account generally, because near the maximum of the focusing the value of the amplitude of the first harmonic becomes comparable with the value of the bias electric field. The using of 3D beams makes possible to increase of the maxima of higher harmonics compared with 2D beams, but the relative values of these maxima are smaller in 3D beams than in 2D ones.

Because the value of the temperature of the crystal is the important parameter to realize the frequency multiplication, it is better to use the input pulses of durations < 1 μs to avoid the heating of crystals.

5. Conclusions

In the lower part of the terahertz range in the nonlinear crystalline paraelectrics like $SrTiO_3$, it is possible to observe the generation of higher harmonics and thus to realize the frequency up-conversion. The crystalline paralectric $SrTiO_3$ possesses the cubic dielectric nonlinearity, so to increase the efficiency of harmonic generation, it is rather better to apply the bias electric field and to get the induced quadratic nonlinearity. In THz range, the frequency dispersion takes place, so the number of harmonics is large but finite, of about 10 - 20. The initial focusing of the beams by the circular antenna results not only in higher efficien-

cy of generation, but also makes possible to select the maxima of different harmonics at specified distances from the input.

The generation of higher harmonics can be realized in the wide temperature range 60 - 200 K. At lower temperatures, the possible frequencies are smaller, of about 0.5 THz, but the nonlinearity is higher. At higher temperatures, the frequency up-conversion can be observed up till the frequencies of about 1.5 THz.

Both plane and cylindrical focused beams can be used for generation of harmonics. In cylindrical beams, the absolute maxima of harmonics can be higher than in plane ones, but the ratios of these maxima to ones of the first harmonic are lower in the cylindrical beams. The influence of the cubic nonlinearity and the zeroth harmonic is essential in the cylindrical beams due to high values of the focused first harmonic.

Acknowledgements

The authors are grateful to SEP-CONAHCyT (Mexico) for a partial support of our work.

Conflicts of Interest

The authors declare no conflicts of interest regarding the publication of this paper.

References

[1] Biswas, A., Banerjee, A., Acharyya, A., Inokawa, H. and Roy, J.N. (2020) Emerging Trends in Terahertz Solid-State Physics and Devices: Sources, Detectors, Advanced Materials, and Light-Matter Interactions. Springer, New York. https://doi.org/10.1007/978-981-15-3235-1

[2] Carpintero, G., Garcıa Muñoz, L.E., Hartnagel, H.L., Preu, S. and Räisänen, A.V. (2015) Semiconductor Terahertz Technology Devices and Systems at Room Temperature Operation. Wiley, New York. https://doi.org/10.1002/9781118920411

[3] Bründermann, E., Hübers, H.-W. and Kimmitt, M.F. (2012) Terahertz Techniques. Springer, New York. https://doi.org/10.1007/978-3-642-02592-1

[4] Song, H.-J. and Nagatsuma, T. (2015) Handbook of Terahertz Technologies. Devices and Applications. CRC Press, Taylor & Francis Group, Boca Raton.

[5] Rieh, J.-S. (2021) Introduction to Terahertz Electronics. Springer, New York. https://doi.org/10.1007/978-3-030-51842-4

[6] Choudhury, B., Rakesh, A.M. and Jha, M. (2016) Active Terahertz Metamaterial for Biomedical Applications. Springer, New York. https://doi.org/10.1007/978-981-287-793-2

[7] Ganichev, S.D. and Prettl, W. (2006) Intense Terahertz Excitation of Semiconductors. Oxford University Press, Oxford. https://doi.org/10.1093/acprof:oso/9780198528302.001.0001

[8] Kolejáka, P., Postava, K., Mičica, M., Kužel, P., Kadlec, F. and Pištora, J. (2018) Experimental Gouy Phase Shift Compensation in Terahertz Time-Domain Spectroscopy. *Photonics and Nanostructures—Fundamentals and Applications*, **31**, 129-133. https://doi.org/10.1016/j.photonics.2018.06.011

[9] Dexheimer, S.L. (2008) Terahertz Spectroscopy Principles and Applications. CRC Press, Boca Raton.

[10] O'Sullivan, C. and Murphy, J.A. (2012) Field Guide to Terahertz Sources, Detectors, and Optics. SPIE Press, Bellingham. https://doi.org/10.1117/3.952851

[11] Perenzoni, M. and Paul, D.J. (2014) Physics and Applications of Terahertz Radiation. Springer, New York. https://doi.org/10.1007/978-94-007-3837-9

[12] Siegel, P.H. (2002) Terahertz Technology. *IEEE Transactions on Microwave Theory and Techniques*, **50**, 910-928. https://doi.org/10.1109/22.989974

[13] Mittleman, D. (2003) Sensing with Terahertz Radiation. Springer, New York. https://doi.org/10.1007/978-3-540-45601-8

[14] Atakaramians, S., Shahraam Afshar, V., Monro, T.M. and Abbott, D. (2013) Terahertz Dielectric Waveguides. *Advances in Optics and Photonics*, **5**, 169-215. https://doi.org/10.1364/AOP.5.000169

[15] Woolard, D.L., Loerop, W.R. and Shur, M.S. (2003) Terahertz Sensing Technology, 2 Vols. World Scientific Publ., Singapore. https://doi.org/10.1142/5244

[16] Lee, Y.-S. (2009) Principles of Terahertz Science and Technology. Springer, New York.

[17] Robertson, W.M. (1995) Optoelectronic Techniques for Microwave and Millimeter-Wave Engineering. Artech Publ., Norwood.

[18] Gevorgian, S. (2009) Ferroelectrics in Microwave Devices, Circuits and Systems. Springer, New York. https://doi.org/10.1007/978-1-84882-507-9

[19] Vendik, O.G. (1979) Ferroelectrics in Microwave Technology. Sov. Radio, Moscow. (In Russian)

[20] Vendik, O.G. and Zubko, S.P. (1997) Phenomenological Description of the Permittivity of Strontium Titanate as a Function of Applied Electric Field and Temperature. *Technical Physics*, **42**, 278-281. https://doi.org/10.1134/1.1258678

[21] Blinc, R. and Žekš, B. (1974) Soft Modes in Ferroelectrics and Antiferroelectrics. North-Holland, Amsterdam.

[22] Lines, M.E. and Glass, A.M. (1977) Principles and Applications of Ferroelectric and Related Materials. Clarendon Press, Oxford.

[23] Rabe, K.M., Ahn, C.H. and Triscone, J.-M. (2007) Physics of Ferroelectrics. A Modern Perspective. Springer, New York.

[24] Strukov, B.A. and Levanyuk, A.P. (1998) Ferroelectric Phenomena in Crystals. Springer, New York. https://doi.org/10.1007/978-3-642-60293-1

[25] Maugin, G.A. (1988) Continuum Mechanics of Electromagnetic Solids. North-Holland, Amsterdam.

[26] Buzin, I.M., Ivanov, I.V., Belokopytov, G.V., Sychev, V.M. and Chuprakov, V.F. (1981) Low-Temperature Ferroelectrics: Dielectric Permittivity, Losses, and Parametric Interactions at Ultrahigh Frequencies. *Izvestiya VUZ, Fizika*, **24**, 6-28. (English Transl. *Soviet Physics Journal*) https://doi.org/10.1007/BF00941340

[27] Rez, I.S. and Poplavko, Yu.M. (1989) Dielectrics. Basic Properties and Applications in Electronics. Radio and Svyaz', Moscow. (In Russian)

[28] Poplavko, Yu.M., Pereverzeva, L.P., Voronov, S.O. and Yakimenko, Yu.I. (2007) Physical Material Science. Vol. 2. Dielectrics. KPI Publ., Kiev. (In Ukrainian)

[29] Gassanov, L.G., Koshevaya, S.V., Narytnik, T.N. and Omel'yanenko, M.Yu. (1978) Parametric and Nonlinear Interaction of Electromagnetic Waves in Paraelectrics. *Izv VUZ Radioelektronika*, **21**, 56-63. (English Transl. *Radioelectronics and Com-*

munications Systems)

[30] Gassanov, L.G., Koshevaya, S.V. and Omel'yanenko, M.Yu. (1980) On Frequency Multiplication in Paraelectrics. *Radiotekhnika i Elektronika*, **25**, 1238-1243. (English Transl. *Radio Engineering and Electronic Physics*)

[31] Koshevaya, S.V., Kononov, M.V. and Omel'yanenko, M.Yu. (1985) An Influence of Dispersion in Waveguiding Systems with Cubically Nonlinear Dielectrics. *Izv VUZ Radioelektronika*, **28**, 53-56. (English Transl. *Radioelectronics and Communications Systems*)

[32] Koshevaya, S.V., Grimalsky, V.V., Kotsarenko, Y.N. and Tecpoyotl-T, M. (2016) Modulation Instability of Transversely Limited Electromagnetic Waves of Terahertz Range in Strontium Titanate Paraelectric. *Radioelectronics and Communications Systems*, **59**, 489-495. https://doi.org/10.3103/S0735272716110029

[33] Grimalsky, V., Koshevaya, S., Escobedo-Alatorre, J. and Tecpoyotl-Torres, M. (2016) Nonlinear Terahertz Electromagnetic Waves in $SrTiO_3$ Crystals under Focusing. *Journal of Electromagnetic Analysis and Applications* (*JEMAA*), **8**, 226-239. https://doi.org/10.4236/jemaa.2016.810021

[34] Grimalsky, V., Koshevaya, S., Escobedo-Alatorre, J. and Jatirian-Foltides, E. (2017) Formation of Short Terahertz Electromagnetic Pulses in Nonlinear Paraelectrics. *Proceedings* 30*th International Conference on Microelectronics MIEL*-2017, Nis, 9-11 October 2017, 91-94. https://doi.org/10.1109/MIEL.2017.8190076

[35] Grimalsky, V., Koshevaya, S., Escobedo-Alatorre, J. and Jatirian-Foltides, E. (2019) Stimulated Brillouin Scattering of Terahertz Electromagnetic Pulses in Paraelectrics. *Applied Physics B*, **125**, 15-22. https://doi.org/10.1007/s00340-018-7125-4

[36] Grimalsky, V.V., Rapoport, Y.G., Boardman, A.D. and Koshevaya, S.V. (2018) Nonlinear Focusing of Picosecond Baseband Pulses in Paraelectric Crystals. *Optical and Quantum Electronics*, **50**, 102-114. https://doi.org/10.1007/s11082-018-1369-4

[37] Grimalsky, V.V., Rapoport, Yu.G., Koshevaya, S.V., Escobedo-Alatorre, J. and Tecpoyotl-Torres, M. (2021) Nonlinear Focusing of Picosecond Baseband Pulses in Paraelectric Crystals in a Wide Temperature Range. *Optical and Quantum Electronics*, **53**, Paper 484. https://doi.org/10.1007/s11082-021-03104-6

[38] Rapoport, Yu.G., Grimalsky, V.V., Koshevaya, S.V. and Melendez-Isidoro, D.L. (2015) Modulation Instability of Terahertz Electromagnetic Pulses in $SrTiO_3$ Paraelectric. *Proceedings* 2015 *IEEE* 35*th International Conference on Electronics and Nanotechnology* (*ELNANO*), Kyiv, 21-23 April 2015, 131-134. https://doi.org/10.1109/ELNANO.2015.7146851

[39] Zamudio-Lara, A., Koshevaya, S.V., Grimalsky, V.V. and Yañez-Cortes, F. (2015) Frequency Multiplication of Terahertz Radiation in the Crystals of Strontium Titanate Paraelectric. *Radioelectronics and Communications Systems* (*Izvestiya VUZ*, *Radioelektronika*), **58**, 411-416. https://doi.org/10.3103/S0735272715090034

[40] Kozina, M., Fechner, M., Marsik, P., *et al.* (2019) Terahertz-Driven Phonon Upconversion in $SrTiO_3$. *Nature Physics*, **15**, 387-392. https://doi.org/10.1038/s41567-018-0408-1

[41] Kamarás, K., Barth, K.L., Keilmann, F., Henn, R., Reedyk, M., Thomsen, C., Cardona, M., Kircher, J., Richards, P.L. and Stehle, J.L. (1995) The Low Temperature Infrared Optical Functions of $SrTiO_3$ Determined by Refectance Spectroscopy and Spectroscopic Ellipsometry. *Journal of Applied Physics*, **78**, 1235-1240. https://doi.org/10.1063/1.360364

[42] Yashchyshyn, Y., Godziszewski, K., Bajurko, P., Modelski, J., Szafran, M., Bobryk, E., Pawlikowska, E., Tarapata, G., Weremczuk, J. and Jachowicz, R. (2013) Tunable

Ferroelectric Ceramic-Polymer Composites for Sub-THz Applications. *Proceedings* 43*rd European Microwave Conference*, Nuremberg, 7-10 October, 2013, 676-679. https://ieeexplore.ieee.org/document/6686746 https://doi.org/10.1109/APMC.2013.6695095

[43] Bloembergen, N. (1965) Nonlinear Optics. W. A. Benjamin Inc., New York.

[44] Kivshar, Y.S. and Agrawal, G.P. (2003) Optical Solitons. From Fibers to Photonic Crystals. Academic Press, New York. https://doi.org/10.1016/B978-012410590-4/50012-7

[45] Weiland, J. and Wilhelmsson, H. (1977) Coherent Non-Linear Interaction of Waves in Plasmas. Pergamon Press, London. https://doi.org/10.1007/978-1-4757-1571-2_29

[46] Samarskii, A.A. (2001) The Theory of Difference Schemes. Marcel Dekker Inc., New York. https://doi.org/10.1201/9780203908518